

Synthesis, characterization and relative catalytic study of ZrO_x - $MnCO_3$, – MnO_2 or $-Mn_2O_3$ deposited on highly reduced graphene oxide nanocomposites for aerobic oxidation of secondary alcohols

Mohamed E Assal¹, Mohammed Rafi Shaik¹, Mufsir Kuniyil^{1,2}, Mujeeb Khan¹, Abdulrahman Al-Warthan¹, Mohammed Rafiq H Siddiqui¹, Joselito P Labis³, RaviVarala⁴ & Syed Farooq Adil^{*1}

¹Department of Chemistry, College of Science, King Saud University, Riyadh 114 51, Kingdom of Saudi Arabia.

²Department of Chemistry, K L University, Guntur 522 502, Andhra Pradesh, India.

³King Abdullah Institute for Nanotechnology, King Saud University, Riyadh 114 51, Kingdom of Saudi Arabia

⁴Department of Chemistry, RGUKT-Basar, Mudhole, Adilabad 504 107, Telangana, India.

E-mail: sfadil@ksu.edu.sa

Received 23 November 2017; accepted 13 July 2018

Zirconia nanoparticles doped $MnCO_3$ have been successfully immobilized on various percentages of highly reduced graphene oxide (HRG)[(X%)HRG/ $MnCO_3$ –(1%) ZrO_x](where, X=0–7), via a facile and straight forward co-precipitation method. Upon calcination, the as-obtained materials have yielded different types of HRG/manganese oxide nanocomposites at different temperatures i.e. [(X%)HRG/ MnO_2 –(1%) ZrO_x] and [(X%)HRG/ Mn_2O_3 –(1%) ZrO_x]. A detail investigation was carried out to compare the catalytic performance of carbonates and oxides based nanocomposites for the selective oxidation of secondary alcohols. For this purpose, molecular oxygen was employed as an environmentally benign oxidant under base-free conditions. The reaction conditions were optimized with different weight percentages of HRG, reaction times, calcination temperatures, catalyst dosages, and reaction temperatures using 1-phenylethanol as a substrate model. The catalytic performance of the nanocomposites was enhanced significantly due to the presence of HRG as a support material. The catalyst with (1%)HRG/ $MnCO_3$ –(1%) ZrO_x exhibited outstanding performance as well as excellent selectivity in the aerobic oxidation of 1-phenylethanol. In this case, 100% conversion in 4 min with more than 99% selectivity was achieved with excellent specific activity of $60.0 \text{ mmol.g}^{-1}.\text{h}^{-1}$. Moreover, catalyst can be efficiently reused 5 times without discernible decrease in its activity and selectivity. Apart from this, various other alcohols were also selectively oxidized to their corresponding carbonyls with complete conversion in short reaction times under optimal conditions without over-oxidation to the carboxylic acids.

Keywords: Alcohols, Catalyst, Highly reduced graphene, Oxidation, Zirconia.

The selective oxidation of alcohols into their resultant aldehydes or ketones is one of the most significant transformations in organic chemistry^{1,2}. The oxidation products are important precursors and intermediates in the perfumery, confectionary, flame-retardants, biofuels, cosmetics, insecticides, and pharmaceutical industries^{3,4}. Usually, the oxidation of alcohols has been carried out using stoichiometric amounts of expensive, toxic, and corrosive oxidants such as pyridinium chlorochromate (PCC), pyridinium dichromate (PDC), TBHP (tert-butyl hydroperoxide), dichromate, chromium trioxide, and potassium permanganate⁵. These methods are environmentally undesirable because of the production of lots of toxic wastes and high costs⁶. Recently, eco-friendly oxidants such as molecular oxygen have been extensively utilized in alcohol oxidation, as it offers various benefits such as, it is abundant in nature, low

cost, environmentally benign, and only produces water as the by-product⁷. In this regard, plethora of studies have been reported using noble metals such as Au⁸, Pd⁹, Pt¹⁰, Ru¹¹, and Rh¹² as a heterogeneous catalyst for the selective oxidation of alcohols with high catalytic activity and selectivity. However, these catalysts possess several drawbacks including high-cost, difficulty in preparation, and rarity of the noble metals which greatly effects the industrial applications of these catalysts¹³. Thus, considerable efforts have been made to replace these precious noble metals with low-cost and abundant non-noble metals, e.g., copper¹⁴, cobalt¹⁵, nickel¹⁶, iron¹⁷, vanadium¹⁸, silver¹⁹, chromium²⁰, molybdenum²¹, rhenium²² and zinc²³ for catalytic oxidation of alcohols. In this regard, various metal and/or metal oxide nanocatalysts were also found to be highly effective and efficient for the selective oxidation of alcohols. Moreover, it is widely

reported that the catalytic performance of these mixed metal oxide nanocatalysts can be remarkably improved by doping with other metals, which typically enhance the surface of the nanocatalysts²⁴. Among various metal oxide nanoparticles, manganese dioxide (MnO_2) was found to be highly active for catalytic oxidation of alcohols to corresponding carbonyls, due to its high stability²⁵. Apart from this, it is low cost and environmental friendly²⁶. Therefore, several types of manganese oxide, mixed manganese oxide, noble metal doped/supported Mn oxides have been extensively employed for the selective oxidation of several organic compounds. For instance, oxidation of naphthalene²⁷, carbon monoxide²⁸, toluene²⁹, ethylene and propylene³⁰, cyclohexane³¹, alkyl aromatics³² and formaldehyde³³.

Graphene is a unique material consisting of a single layer of sp^2 hybridized carbon atoms in a densely packed honeycomb two-dimensional (2D) lattice³⁴. Since the discovery of mono-layer graphene via mechanical exfoliation of graphite, number of publications employing graphene for various applications have been exploded³⁵. Due to the unique physicochemical properties of graphene, the graphene-based materials possess outstanding catalytic, magnetic and electronic properties that have exploited for several applications such as energy storage, drug delivery, lithium ion batteries, gas storage, water purification, sensors, super capacitor, solar cells, and catalysis³⁶⁻³⁸. Recently, graphene and graphene-based materials have gained growing interests as promising materials as catalyst supports in oxidation reactions due to presence of oxygenic functional groups as well as carbon vacancies and topological defects on their surfaces. These groups promotes and enhance the possibility of sorption and intercalation of ions which ultimately increase the catalytic activity of the material³⁹. Besides, the resulting metal and/or metal oxide nanocomposites of HRG also possess large specific surface area which enabled them to functioned as efficient catalysts several chemical transformations, e.g. Suzuki coupling reaction⁴⁰, of benzylic alcohols reduction⁴¹, ammonia borane dehydrogenation⁴², CO oxidation⁴³, synthesis of aniline⁴⁴, and methanol oxidation⁴⁵. Particularly, these materials have been prominently used as an efficient catalyst for the catalytic oxidation of alcohols into their corresponding aldehydes and ketones, e.g. PdNPs/GC⁴⁶, $\gamma\text{-MnO}_2/\text{GO}$ ⁴⁷, AgNPs/HRG⁴⁸, Au/HRG⁴⁹, Pt/HRG⁵⁰, $\text{Fe}_3\text{O}_4\text{-Pt/HRG}$ ⁵¹ and TiO_2/HRG ⁵².

Continuing our interest in using several mixed metal oxide nanoparticles as an efficient catalyst for the aerial oxidation of alcohols into corresponding aldehydes and ketones⁵³⁻⁵⁵, herein, we present a comparative study between the catalytic performance of ZrO_xNPs doped MnCO_3 with/without carbon support and the role of support toward the aerobic oxidation of secondary alcohols to their corresponding ketones. The nanocomposites were prepared by a facile co-precipitation method and were characterized by various techniques including, scanning electron microscopy (SEM), energy-dispersive X-ray spectroscopy (EDX), powder X-ray diffraction (XRD), thermal gravimetric analysis (TGA), Brunauer-Emmett-Teller (BET), Raman spectroscopy and Fourier transform infrared spectroscopy (FT-IR). The catalytic activities of the as-prepared nanocomposites were evaluated for the selective oxidation of alcohols in presence of molecular O_2 as a green oxidizing agent. To the best of our knowledge, this is the first study on using HRG as a support material for ZrO_xNPs doped MnCO_3 to produce graphene based $\text{ZrO}_x\text{NPs}/\text{MnCO}_3$ as a catalyst for aerobic oxidation of secondary alcohols.

Experimental Section

Materials

Manganese(II) nitrate tetrahydrate (97%), Zirconium nitrate (99%), Sodium bicarbonate (99%), Toluene (98%), Benzyl alcohol (99.5%), Biphenyl 4 methanol (98%), 2-Phenylethanol (98%), Furfuryl alcohol (98%), Cinnamyl alcohol (98%), Diphenylmethanol (99%), 4-Chlorobenzhydrol (98%), 1-Phenylethanol (98%), 1(4 Chlorophenyl)ethanol (98%), 1-Phenyl 2-propanol (98%), 4-Phenyl 2-butanol (97%), Cyclohexanemethanol (99%), 1-Octanol (99%), 5-Hexen-1-ol (98%), β Citronellol (98%), Cyclohexanol (99%), 3-Buten 2-ol (97%), 2-Octanol (99%), Potassium permanganate (99%), Hydrazine hydrate, Sodium nitrate, and Hydrogen peroxide were purchased from Sigma Aldrich, St. Louis, MO 63118, USA. Graphite powder was purchased from Alfa Aesar.

Preparation of highly reduced graphene oxide (HRG)

Firstly, graphene oxide (GO) is synthesized from graphite by the modified Hummers method⁵⁶. To obtain HRG, graphene oxide (200 mg) is dispersed in 40 mL distilled water and sonicated for 30 min. The suspension is heated to 100°C and subsequently 6 mL of hydrazine hydrate is added into it. It is then allowed to stir at 98°C for 24 h. Thereafter, HRG was collected by filtration in the form of black powder.

The obtained material was washed using distilled water for several times to remove the excessive hydrazine and redistributed into water by sonication. Finally, the suspension was centrifuged at 4000 rpm for 3 min to remove bulk graphite and the product was collected and dried in vacuum.

Preparation of (X%) HRG/MnCO₃-(1%)ZrO_x catalysts

The (X%)HRG/MnCO₃-(1%)ZrO_x catalysts were synthesized by co-precipitation method (where X = 0, 1, 3, 5 and 7). In a typical synthesis stoichiometric amount of manganese (II) nitrate-tetra-hydrate (Mn(NO₃)₂.4H₂O) and zirconium nitrate (Zr(NO₃)₂) and highly reduced graphene oxide (HRG) were mixed in a round bottomed flask and subjected to ultrasonication for 30 min. Then, the resulting solution was heated to 80°C, while vigorously stirring using a mechanical stirrer and 0.5 M solution of sodium bicarbonate (NaHCO₃), was added drop wise by using burette until the solution attained at pH 9. The solution was continued to stir at the same temperature for about 3 h and then left under stirring over night at room temperature. The solution was filtered using a Buchner funnel under vacuum and then dried at 70°C overnight in the oven. The resulting powder was then calcined at various temperatures (i.e. 300, 400 and 500 °C) (Scheme 1).

Catalyst characterization

Scanning electron microscopy (SEM) was carried out using Jeol SEM model JSM 6360A (Japan) and elemental analysis (Energy Dispersive X-Ray Analysis: EDX) were carried out using Jeol SEM model JSM 6360A (Japan). This was used to determine the morphology of nanoparticles Powder

X-ray diffraction studies were carried out using Altima IV [Make: Regaku] X-ray diffractometer. Fourier Transform Infrared Spectroscopy (FT-IR) the infrared spectra were recorded as KBr pellets using a Perkin-Elmer 1000 FT-IR spectrophotometer. BET surface area was measured on a NOVA 4200e surface area & pore size analyzer. Thermogravimetric analysis was carried out using Perkin-Elmer Thermogravimetric Analyzer 7.

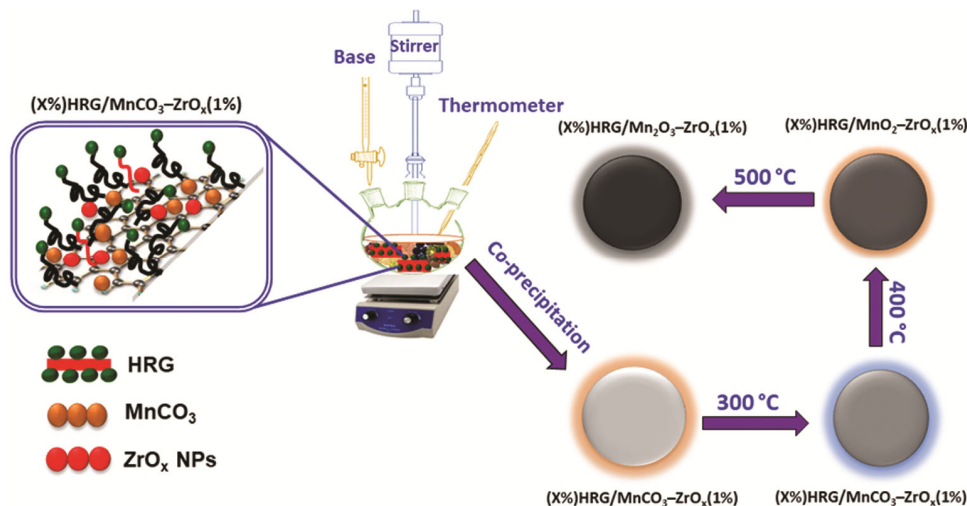
General procedure of oxidation of alcohols

Liquid-phase oxidation of 1-phenylethanol as example of secondary aromatic alcohols has performed in glass flask equipped with a magnetic stirrer, reflux condenser, and thermometer. In a typical experiment, a mixture of the 1-phenylethanol (2 mmol), toluene (10 mL), and the catalyst (300 mg) was transferred in a glass three-necked round-bottomed flask (100 mL); the resulting mixture was then heated to desired temperature with vigorous stirring. The oxidation experiment was started by bubbling oxygen gas at a flow rate of 20 mL.min⁻¹ into the reaction mixture. After the reaction, the solid catalyst was filtered off by centrifugation and the liquid products were analyzed by gas chromatography to determine the conversion of the alcohol and product selectivity by (GC, 7890A) Agilent Technologies Inc, equipped with a flame ionization detector (FID) and a 19019S-001 HP-PONA column.

Results and Discussion

FT-IR spectrometer

FT-IR spectra of the graphene oxide (GO), highly reduced graphene (HRG), and (1%)HRG/MnCO₃-(1%)ZrO_x samples are displayed in Fig. 1. The FT-IR



Scheme 1 — Synthetic illustration of the as-synthesized catalyst at different calcination temperatures.

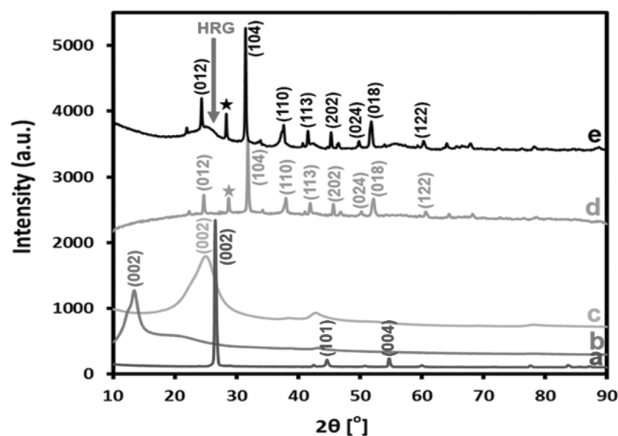


Fig. 1 — FT-IR spectra of (a) GO, (b) HRG, and (c) (1%)HRG/MnCO₃-(1%)ZrO_x.

spectrum of GO (Fig. 1a) displays a broad peak at $\sim 3440\text{ cm}^{-1}$ due to the stretching of hydroxyl groups (O-H) present on the surface of GO, the absorption band at 1740 cm^{-1} is accompanying with (C=O) stretching of carboxylic groups (-COOH) on the surface⁵⁷, and the peak at 1630 cm^{-1} is allocated to the stretching vibration of carbon backbone (C=C/C-C) from unoxidized graphite lattice⁵⁸. The absorption peaks at 1395 , 1227 , 1065 cm^{-1} are associated to stretching vibrations of (C-OH), (C-O-C) epoxy and (C-O) alkoxy, respectively⁵⁹. For HRG (Fig. 1b), the broad absorptions peak at 1214 cm^{-1} is attributed to (C-OH) stretching vibration and weak peak around 1634 cm^{-1} is related with (C=C) group due to the skeletal aromatic vibration, other peaks cannot be clearly identified⁵⁷. Nevertheless, the comparison between the FT-IR spectra of GO with (1%)HRG/MnCO₃-(1%)ZrO_x nanocomposite evidently exhibits significant reduction of majority of the oxygenated groups on the surface of the GO. The strong intense peaks at 1740 , 1225 , and 1060 cm^{-1} correlated to (C=O), (C-O-C), and (C-O) stretching vibrations cannot be noticed by comparing with GO, specifying that the oxygen containing functional groups on GO surfaces were almost eradicated. The FT-IR spectra of (1%)HRG/MnCO₃-(1%)ZrO_x is dominated by a peak at 1634 cm^{-1} resultant to (C=C) stretching modes allocated to the skeletal aromatic vibration and wide absorption peak belonging to carbonate groups were observed at 1380 cm^{-1} (Fig. 1c)⁶⁰. The intense sharp absorption peak situated nearly at 590 cm^{-1} is allocated to Mn-O vibrations⁴⁷.

X-ray diffraction (XRD)

The XRD patterns of the graphite powder, graphene oxide (GO) highly reduced graphene

oxide (HRG), unsupported MnCO₃-(1%)ZrO_x, and (1%)HRG/MnCO₃-(1%)ZrO_x nanocomposite are displayed in Fig. 2. The XRD patterns of the pristine graphite displayed a sharp and single diffraction line at $2\theta = 26.5^\circ$ which resembles to the diffraction peak at (002) plane with a d-spacing of 3.37 \AA as described in Fig. 2a⁶¹. Nevertheless, graphene oxide (GO) shows the diffraction peak at $2\theta = 11.8^\circ$. The vanishing of the graphite peak at $2\theta = 26.5^\circ$ and presence of a new peak at $2\theta = 11.8^\circ$ can be attributed to the emergence of graphene oxide upon graphite oxidation (Fig. 2b)⁴¹. This shift leads to an increase in interlayer spacing value from 3.37 to 6.41 \AA for graphite and graphene oxide correspondingly, which clearly indicates the introduction of different oxygen containing functionalities between the graphite layers during the oxidation process. XRD pattern of HRG exhibits broad diffraction peak at $2\theta = 24.5^\circ$ which is a characteristic peak of HRG and point toward the reduction of GO⁶². As estimated, in the XRD pattern (1%)HRG/MnCO₃-(1%)ZrO_x catalyst (Fig. 2c), the characteristic diffraction peak of GO at $2\theta = 11.8^\circ$ was not observed and the existence of broad peak at about $2\theta = 24.5^\circ$, confirmed the complete reduction of GO to HRG. Moreover, the XRD pattern of unsupported MnCO₃-(1%)ZrO_x exhibits that lack of the characteristic broad peak of HRG at $2\theta = 24.5^\circ$ as illustrated in Fig. 2d. In addition, XRD pattern of MnCO₃-(1%)ZrO_x exhibited a rhodochrosites manganese carbonate oxides (JCPDS No. 00-001-0981) [space group R-3c (167)]. The (1%)HRG/MnCO₃-(1%)ZrO_x catalyst shows a similar XRD pattern as MnCO₃-(1%)ZrO_x. The absorption peaks marked with (*) could be attributed to the existence of ZrO_x (monoclinic phase) in both MnCO₃-(1%)ZrO_x as well as (1%)HRG/MnCO₃-(1%)ZrO_x nanocomposite.

Thermal stability

Thermogravimetric analysis (TGA) endorses that whole transformation of graphene oxide to HRG nano-sheets under reduction with hydrazine hydrate as reducing agents and offer the evidence about the thermal stability of the as-synthesized catalyst. Figure 3 exhibits the TGA patterns for the graphite, graphene oxide, highly reduced graphene oxide, MnCO₃-(1%)ZrO_x and (1%)HRG/MnCO₃-(1%)ZrO_x samples. As displayed in Fig. 3, the thermal stability of graphene oxide is much lesser than the pristine graphite⁶³. The attained thermogram for pristine graphite demonstrate that it undergoes a total weight loss of $\sim 1\%$ (Fig. 3a)⁶⁴, while graphene oxide exhibits

a weight loss of $\sim 65\%$ (Fig. 3b), which is very much in agreement with the formerly stated literature⁵⁸. The highly reduced graphene oxide (HRG) TGA curve displayed overall weight loss of nearby 20% at the same temperature range due to the reduction of the oxygen containing functional groups as shown Fig. 3c. The (1%)HRG/ $MnCO_3$ -(1%) ZrO_x nanocomposite exhibited an aggregate weight loss less than 18% in the identical temperature range (Fig. 3e), which is marginally in excess of the weight loss evident from the degradation pattern of $MnCO_3$ -(1%) ZrO_x signifying that effective reduction of graphene oxide to HRG by eradicating maximum of the oxygen carrying functionalities such as carboxyl, hydroxyl, epoxy, and carbonyl groups⁴².

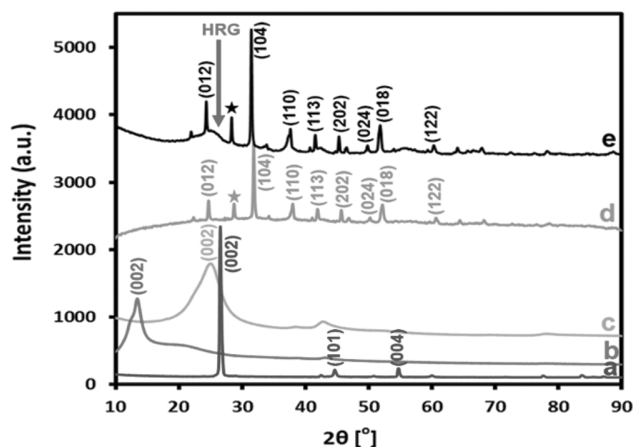


Fig. 2 — XRD patterns of the (a) graphite, (b) GO, (c) HRG, (d) $MnCO_3$ -(1%) ZrO_x , and (e) (1%)HRG/ $MnCO_3$ -(1%) ZrO_x nanocomposite.

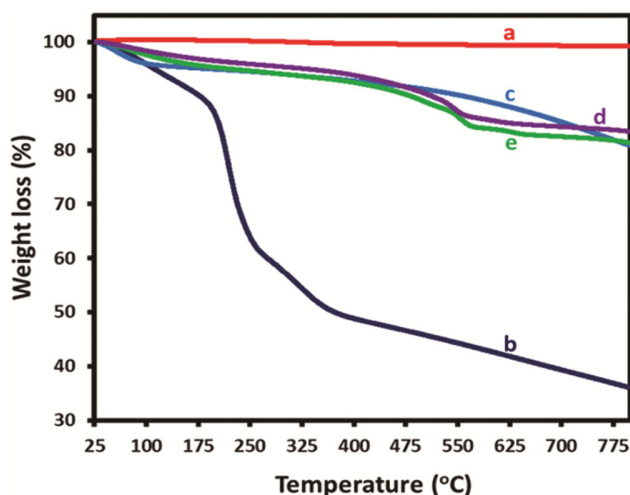


Fig. 3 — TGA curves of (a) graphite, (b) graphene oxide (GO), (c) highly reduced graphene oxide (HRG), (d) $MnCO_3$ -(1%) ZrO_x , and (e) (1%)HRG/ $MnCO_3$ -(1%) ZrO_x .

Raman spectroscopy

Raman spectroscopy is an informative technique, which is effectively used to study graphene-based nanocomposites. Figure 4 shows the Raman spectra of GO, $MnCO_3$ -(1%) ZrO_x and (1%)HRG/ $MnCO_3$ -(1%) ZrO_x nanocomposite. Two characteristic peaks at 725 and 1080 cm^{-1} which are attributed to $MnCO_3$ were also present in both $MnCO_3$ -(1%) ZrO_x and (1%)HRG/ $MnCO_3$ -(1%) ZrO_x catalyst, which indicates the occurrence of $MnCO_3$ in the nanocomposite as shown in Fig. 4(b,c)⁶⁵. Moreover, the occurrence of highly reduced graphene oxide in the (1%)HRG/ $MnCO_3$ -(1%) ZrO_x nanocomposite is confirmed by the presence of two main peaks around at 1580 and 1350 cm^{-1} respectively, usually denoted as D band and G-band (Fig. 4c)⁴⁶. The D band is associated to the disorder carbon structure induced by lattice defects and the G-band is accompanying to well-ordered structure. Figure 4a shows a GO spectrum, the G and the D bands are shifted and appear at 1605 and 1346 cm^{-1} correspondingly, due to the destruction of the sp^2 character by the oxidation process and present of oxygen containing functional groups⁶⁶. The characteristic G peak in (1%)HRG/ $MnCO_3$ -(1%) ZrO_x is shifted by $\sim 12\text{ cm}^{-1}$ from 1605 to 1593 cm^{-1} , however a slight shift was observed in the D band from 1346 to 1339 cm^{-1} , which is a clear indication of the reduction of GO to HRG⁶⁷.

Scanning electron microscopy (SEM)

The size and morphology of the as-prepared $MnCO_3$ -(1%) ZrO_x and highly reduced graphene oxide

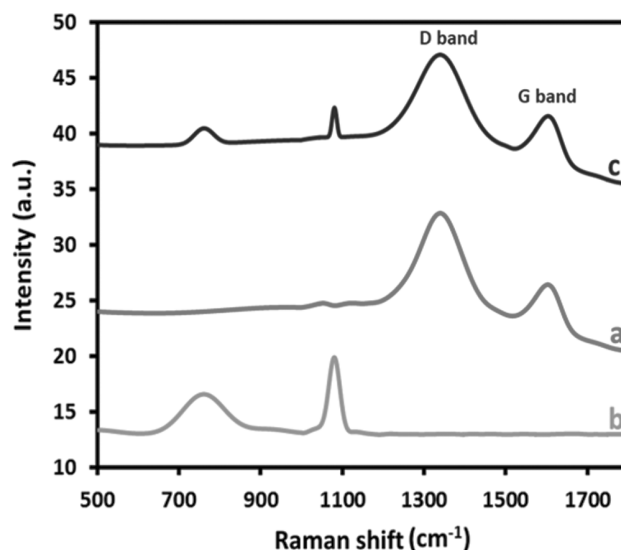


Fig. 4 — Raman spectra of (a) GO, (b) $MnCO_3$ -(1%) ZrO_x , and (c) (1%)HRG/ $MnCO_3$ -(1%) ZrO_x nanocomposite.

supported (1%)HRG/MnCO₃–(1%)ZrO_x catalyst obtained by co-precipitation method is monitored by using scanning electron microscopy (SEM). Figure 5 shows the SEM micrographs of the pure MnCO₃–(1%)ZrO_x after calcining at temperatures 300°C (Fig. 5a) and HRG supported (1%)HRG/MnCO₃–(1%)ZrO_x (Fig. 5b). The pure MnCO₃–(1%)ZrO_x catalyst show micro size but well-defined cuboidal shape particles but HRG supported (1%)HRG/MnCO₃–(1%)ZrO_x (Fig. 5b), interesting shows aggregation of rather smaller size crystals which looks like grown on the surface through proper surface nucleation/growth process. The composition of the catalyst is determined using EDX and stays within experimental error to the theoretical composition (Table 1).

Surface-area analysis (BET)

The surface area of as-fabricated catalysts using BET surface area measurements was examined in order to understand the influence of the surface area of the as-fabricated catalysts on the effectiveness of the catalytic system for oxidation of secondary alcohols. Table 3 clearly displayed that the specific surface areas of the catalysts MnCO₃–(1%)ZrO_x, MnO₂–(1%)ZrO_x, and Mn₂O₃–(1%)ZrO_x without HRG support was about 133.6, 53.2, and 17.5 m².g⁻¹ respectively. Whereas, after using graphene support, the surface areas of the (1%)HRG/MnCO₃–(1%)ZrO_x, (1%)HRG/MnO₂–(1%)ZrO_x, and (1%)HRG/Mn₂O₃–

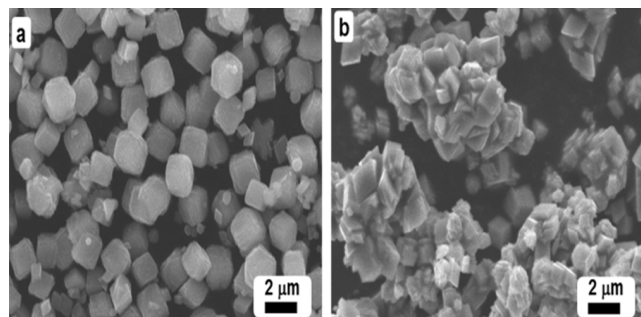


Fig. 5 — SEM images of (a) MnCO₃–(1%)ZrO_x, and (b) (1%)HRG/MnCO₃–(1%)ZrO_x nanocomposite.

Table 1 — The elemental composition of the as-synthesized catalyst (1%)HRG/MnCO₃–(1%)ZrO_x.

Compound	Element Mass (%)			
	C	O	Mn	Zr
MnCO ₃ –(1%)ZrO _x	29.97	15.84	53.24	0.95
(1%)HRG/MnCO ₃ –(1%)ZrO _x	35.07	18.38	45.3	1.25

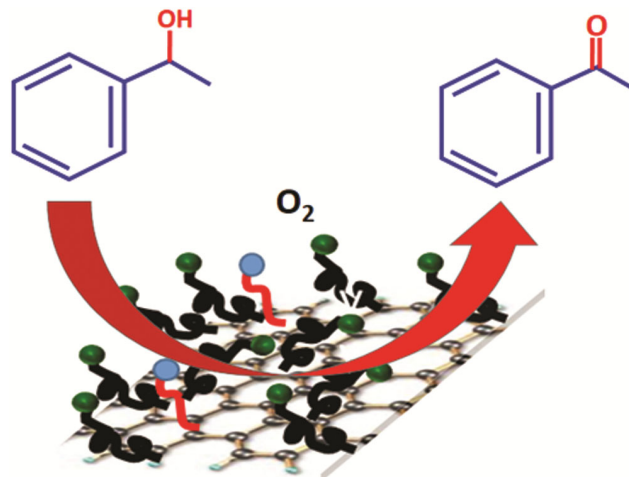
(1%)ZrO_x nanocomposites were increased to 239.1, 179.3, and 131.1 m².g⁻¹ respectively. As expected, after using HRG support the conversion of 1-phenylethanol for the catalysts (1%)HRG/MnCO₃–(1%)ZrO_x, (1%)HRG/MnO₂–(1%)ZrO_x, and (1%)HRG/Mn₂O₃–(1%)ZrO_x have also increased. The considerable increase in the conversion of 1-phenylethanol, probably partially owing to the increment of the surface area of HRG support. It can be concluded from the above finding that the HRG support and surface area play a crucial role in enhancing the oxidation rate. On the hand, The (1%)HRG/MnCO₃–(1%)ZrO_x calcined at 300°C exhibited higher catalytic performance and surface area compared to the catalysts calcined at 400 and 500°C i.e. (1%)HRG/MnO₂–(1%)ZrO_x, and (1%)HRG/Mn₂O₃–(1%)ZrO_x, indicating that the surface area and calcination treatment had a considerable effect in the oxidation of alcohols.

Catalytic evaluation

In order to evaluate the catalytic properties of the prepared nanocomposites, the oxidation of 1-phenylethanol to acetophenone using molecular O₂ is selected as a representative reaction (Scheme 2). The influence of several parameters such as calcination temperature, catalyst loading, catalyst amount, reaction time, and reaction temperature were thoroughly studied in detail in order to optimize the reaction circumstances, as illustrated in Tables 2-5.

Influence of HRG support

The effect of the graphene support on the performance of the heterogeneous catalysts for the



Scheme 2 — Schematic illustration of aerial oxidation of 1-phenylethanol to acetophenone using the as-prepared catalyst.

alcohol oxidation have extensively studied in the literature^{46,48,49}. From our previous reported work, it was found that ZrO_x acting as a very good promoter to the catalyst MnCO₃, and MnCO₃-(1%)ZrO_x was found to be the best catalyst for the benzyl alcohol oxidation⁶⁸. In the present work, the catalytic activity of graphene (HRG), graphene support (HRG) ZrO_x NPs doped MnCO₃ is examined for the selective oxidation of 1-phenylethanol with molecular O₂. Graphical representation of the results was plotted in Fig. 6 and tabulated in Table 2. It is found that HRG is not active for oxidation of 1-phenylethanol

and yields a negligible alcohol conversion (2.89%) within 7 min at 100°C (Table 2, entry 1). However the nanocomposites with varying % of HRG i.e.(X%)HRG/MnCO₃-(1%)ZrO_x[where X= 0, 1, 3, 5, and 7] for the aerial oxidation of 1-phenylethanol has also been examined. The results displayed that unsupported MnCO₃-(1%)ZrO_x catalyst gave 78.51% conversion of 1-phenylethanol within 7 min(Table 2, entry 2). Whilst, after using 1 wt.% of HRG as a catalyst support, the catalytic activity of (1%)HRG/MnCO₃-(1%)ZrO_x has greatly improved and exhibits a complete conversion of 1-phenylethanol within 7 min of reaction time with very high specific activity 57.14 mmol.g⁻¹.h⁻¹ (Table 2, entry 3).

Further increasing the percentage of HRG such as (3%)HRG/MnCO₃-(1%)ZrO_x, (5%)HRG/MnCO₃-(1%)ZrO_x, and (7%)HRG/MnCO₃-(1%)ZrO_x led to decrease in the alcohol conversion, and yielded in alcohol conversion of 94.87, 81.13, and 67.84%, respectively under similar circumstances (Table 2, entries 4–6). The product selectivity remains (>99) unchanged during all experiments (Table 2, entries 1–6). It is deduced that the highest yields for the conversion of 1-phenylethanol is achieved using 1 wt.% of HRG as a catalyst support for ZrO_x NPs deposited on MnCO₃, i.e. (1%)HRG/MnCO₃-(1%)ZrO_x, within 7 min. (Table 2, entry 3) It also confirm that the HRG plays an essential role as a promising support in the enhancement of catalytic

Table 2 — Catalytic oxidation of 1-phenylethanol with molecular oxygen.

Entry	Catalyst	Conv. (%)	Sp. activity (mmol.g ⁻¹ .h ⁻¹)	Sel. (%)
1	HRG	2.89	1.65	>99
2	MnCO ₃ -(1%)ZrO _x	78.51	44.86	>99
3	(1%)HRG/MnCO ₃ -(1%)ZrO _x	100.0	57.14	>99
4	(3%)HRG/MnCO ₃ -(1%)ZrO _x	94.87	54.21	>99
5	(5%)HRG/MnCO ₃ -(1%)ZrO _x	81.13	46.36	>99
6	(7%)HRG/MnCO ₃ -(1%)ZrO _x	67.84	38.77	>99

Reaction conditions: 2 mmol of 1-phenylethanol, calcination temperature: 300°C, catalyst amount: 300 mg, oxygen flow rate: 20 mL.min⁻¹, reaction temperature: 100°C, solvent: 10 mL of toluene, and reaction time: 7 min.

Table 3 — Catalytic oxidation of 1-phenylethanol in different calcination temperatures.

Entry	Catalyst	T (°C)	SA (m ² .g ⁻¹)	Conv. (%)	Sp. activity (mmol.g ⁻¹ .h ⁻¹)	Sel. (%)
1	MnCO ₃ -(1%)ZrO _x	300	133.6	78.51	44.86	>99
2	MnO ₂ -(1%)ZrO _x	400	53.2	49.08	28.05	>99
3	Mn ₂ O ₃ -(1%)ZrO _x	500	17.5	41.72	23.84	>99
4	(1%)HRG/MnCO ₃ -(1%)ZrO _x	300	211.0	100.0	57.14	>99
5	(1%)HRG/MnO ₂ -(1%)ZrO _x	400	102.7	85.97	49.13	>99
6	(1%)HRG/Mn ₂ O ₃ -(1%)ZrO _x	500	60.5	61.07	34.90	>99

Reaction conditions: 2 mmol of 1-phenylethanol, catalyst amount: 300 mg, oxygen flow rate: 20 mL.min⁻¹, reaction temperature: 100°C, solvent: 10 mL of toluene, and reaction time: 7 min.

Table 4 — Aerobic oxidation of 1-phenylethanol in different reaction temperatures.

Entry	Temperature (°C)	Conv. (%)	Sp. activity (mmol.g ⁻¹ .h ⁻¹)	Sel. (%)
1	20	40.80	23.31	>99
2	40	57.06	32.61	>99
3	60	72.33	41.33	>99
4	80	86.64	49.51	>99
5	100	100.0	57.14	>99

Reaction conditions: catalyst: (1%)HRG/MnCO₃-(1%)ZrO_x, 2 mmol of 1-phenylethanol, calcination temperature: 300°C, catalyst amount: 300 mg, oxygen flow rate: 20 mL.min⁻¹, solvent: 10 mL of toluene, and reaction time: 7 min.

Table 5 — Effect of catalyst dosage on the catalytic performance.

Entry	Catalyst amount (mg)	Conv. (%)	Sp. activity ($\text{mmol.g}^{-1}.\text{h}^{-1}$)	Sel. (%)
1	100	25.35	76.05	>99
2	200	44.6	66.90	>99
3	300	64.97	64.96	>99
4	400	83.52	62.64	>99
5	500	100.0	60.0	>99

Reaction conditions: catalyst: (1%)HRG/MnCO₃–(1%)ZrO_x, 2 mmol of 1-phenylethanol, calcination temperature: 300°C, oxygen flow rate: 20 mL.min⁻¹, reaction temperature: 100°C, solvent: 10 mL of toluene, and reaction time: 4 min.

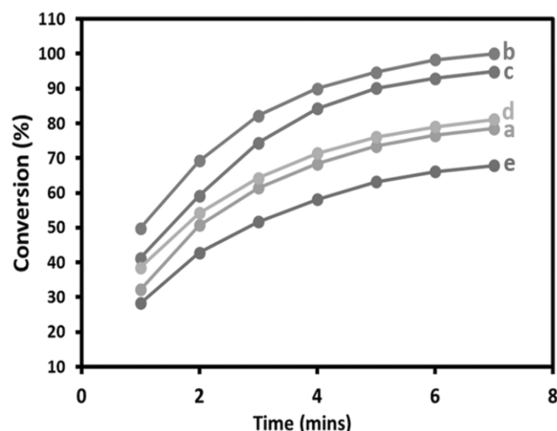


Fig. 6 — Graphical representation of 1-phenylethanol oxidation catalyzed by (a) MnCO₃–(1%)ZrO_x, (b) (1%)HRG/MnCO₃–(1%)ZrO_x, (c) (3%)HRG/MnCO₃–(1%)ZrO_x, (d) (5%)HRG/MnCO₃–(1%)ZrO_x, and (e) (7%)HRG/MnCO₃–(1%)ZrO_x.

performance for the oxidation of 1-phenylethanol. The enhanced catalytic activity after using graphene support, could be due to the large surface area of HRG and presence of various oxygen containing functional groups and other carbon defects that are present on the surface of HRG. These groups not only facilitated the anchoring of nanoparticles and prevent their agglomeration but they also help to hold the reactants on the surface of HRG by π - π stacking and promote the oxidation of alcohols.

The plausible mechanism for catalytic enhancement could be the role of HRG to increase the lifetime of charge carriers, which finally reacts with molecular O₂ to create reactive oxygen species to improve the catalytic oxidation process. Hence, the (1%)HRG/MnCO₃–(1%)ZrO_x nanocomposite was the best among the other catalysts prepared, based on which (1%)HRG/MnCO₃–(1%)ZrO_x catalyst was used in optimize other parameters.

Influence of calcination temperature

The influence of calcination temperature of the catalyst on the catalytic efficiency has investigated in order to get the optimum calcination temperature. The

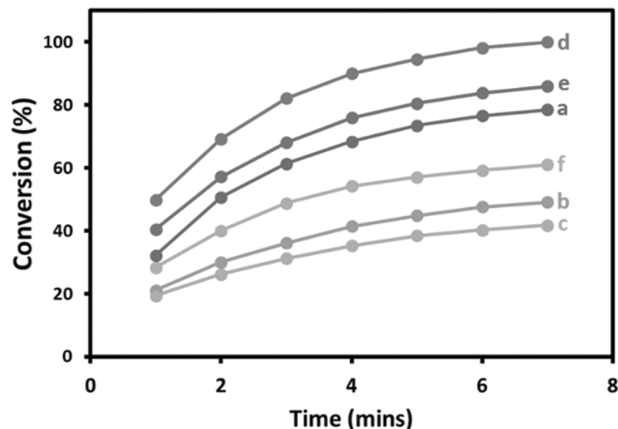


Fig. 7 — Graphical illustration of aerobic oxidation of 1-phenylethanol using the catalysts (a) MnCO₃–(1%)ZrO_x, (b) MnO₂–(1%)ZrO_x, (c) Mn₂O₃–(1%)ZrO_x, (d) (1%)HRG/MnCO₃–(1%)ZrO_x, (e) (1%)HRG/MnO₂–(1%)ZrO_x, and (f) (1%)HRG/Mn₂O₃–(1%)ZrO_x.

catalytic results including alcohol conversion, specific activity, and product selectivity were listed in Table 3 and plotted in Fig. 7. The results indicated that, the calcination temperature have inhibiting effect on this oxidation reaction by decreasing the effectiveness of the catalytic system⁶⁹. The catalyst obtained upon calcination at 400°C i.e. (1%)HRG/MnO₂–(1%)ZrO_x yielded a 85.97% alcohol conversion, while the catalyst calcined at 500°C i.e. (1%)HRG/Mn₂O₃–(1%)ZrO_x, the conversion of 1-phenylethanol reduced to 61.07% (Table 3, entry 6). Whilst, in case of 300°C, the catalyst (1%)HRG/MnCO₃–(1%)ZrO_x showed complete conversion along with 57.14 $\text{mmol.g}^{-1}.\text{h}^{-1}$ specific activity under same reaction conditions (Table 3, entry 4). Additionally, the catalytic activity of the catalysts MnCO₃–(1%)ZrO_x, MnO₂–(1%)ZrO_x, and Mn₂O₃–(1%)ZrO_x without using graphene support (HRG) was also examined and gave only 78.51, 49.08, and 41.72% 1-phenylethanol conversion (Table 3, entries 1–3). Interestingly, the catalytic activity has remarkably improved after using the carbon support (HRG) by

achieving full conversion under similar circumstances within short reaction time. It is worth mentioning, the obtained results consistent with the BET surface area data of the prepared catalyst, which the catalyst (1%)HRG/ $MnCO_3$ -(1%) ZrO_x calcined at 300°C has the highest surface area among all other temperatures and produced a 100% conversion product. Whereas, the catalyst calcined at 400 and 500°C exhibited lower 1-phenylethanol conversion and possess lower surface area. Therefore, it can be said that the catalytic efficiency was strongly effected by calcination temperature and surface area of the catalyst. Although, the product selectivity remained unchanged throughout all the reactions. Hence, we choose to use 300°C as the best calcination temperature in further studies to optimize other parameters.

Influence of reaction temperature

The effect of reaction temperature on the catalytic performance of the (1%)HRG/ $MnCO_3$ -(1%) ZrO_x catalyst for the oxidation of 1-phenylethanol was also explored in the range of 20°C to 100°C, with the results tabulated in Table 4 and depicted in Fig. 8. The conversion of 1-phenylethanol was strongly affected by reaction temperature. At low temperature (20°C), lower conversion of 40.8% was obtained in 7 min (Table 4, entry 1). As expected, the effectiveness of the catalytic system has remarkably enhanced by raising the reaction temperature. The full conversion of 1-phenylethanol was achieved at 100°C with the specific activity of 57.14 $mmol.g^{-1}.h^{-1}$ under identical conditions (Table 4, entry 5). Whereas, the selectivity toward acetophenone still unchanged through all oxidation reactions (above 99%). As a result,

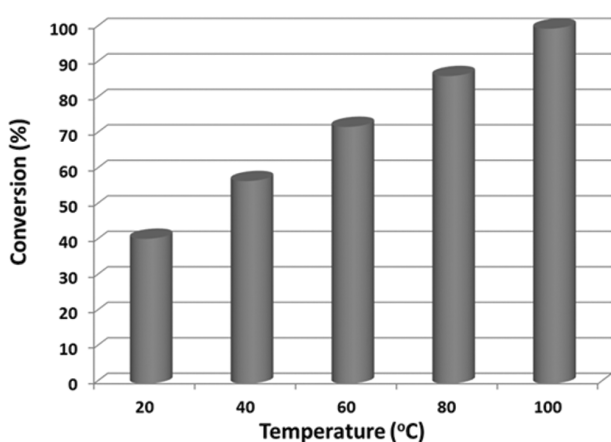


Fig. 8 — Catalytic activity of (1%)HRG/ $MnCO_3$ -(1%) ZrO_x nanocomposite as a function of reaction temperature.

100°C was found to be optimum reaction temperature in this study.

Influence of catalyst dosage

In order to obtain the optimum amount of catalyst for the desired conversion reaction, the oxidation of 1-phenylethanol has carried out using different amounts of the (1%)HRG/ $MnCO_3$ -(1%) ZrO_x nanocomposite. The results related to the catalytic efficiency were described in Table 5 and Fig. 9. Results revealed that, upon increasing the amount of catalyst, the conversion of 1-phenylethanol is also increased, but the product selectivity remained constant (>99%). According to Table 5, when the amount of catalyst increased from 100 mg to 500 mg, the conversion of 1-phenylethanol increased rapidly from 25.35% to 100% within extremely short reaction time (4 min) along with superior specific activity of 60.0 $mmol.g^{-1}.h^{-1}$ (Table 5, entries 1–6). This study demonstrates that, the complete transformation of 1-phenylethanol to acetophenone can be achieved within only 4 min with 500 mg of the catalyst under mild conditions. A linear correlation has found between catalyst amount and conversion of 1-phenylethanol as shown in Fig. 9. In the absence of catalyst, no formation of acetophenone has been detected by GC, indicating that the catalyst is necessary for the oxidation of 1-phenylethanol.

The comparison of catalytic activity of the current catalytic system with previously reported methods was summarized in Table 6 for oxidation of alcohols using several catalysts and different reaction parameters. In the current work, our catalyst afforded a complete conversion and selectivity within very short reaction time 4 min at 100°C and highest

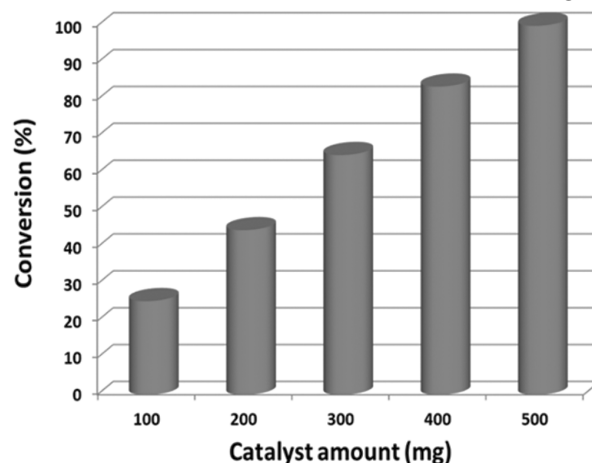


Fig. 9 — Catalytic performance of (1%)HRG/ $MnCO_3$ -(1%) ZrO_x catalyst as a function of catalyst amount.

specific activity ($60\text{mmol.g}^{-1}.\text{h}^{-1}$) by compared with to all other reported catalysts. It can be said that, (1%)HRG/MnCO₃–(1%)ZrO_x catalyst is the most efficient for oxidation of 1-phenylethanol in terms of reaction time and specific activity among all listed catalysts. In contrast, all listed catalysts take extremely long time to completely oxidize the 1-phenylethanol and showed lower specific activity. For an example, Liang *et al.*⁷⁰ have successfully synthesized Au nanoparticles supported on Mg–Al-layered double hydroxide (Au NPs/LDH) and used as a catalyst for selective oxidation of alcohols. The Au NPs/LDH catalyst exhibits complete conversion of 1-phenylethanol and selectivity to acetophenone was nearly 100% along with lower specific activity of $9.28\text{mmol.g}^{-1}.\text{h}^{-1}$ within relatively long reaction time 2 h with respect to our catalyst. In 2016, Wang and co-workers⁷¹ have fabricated Na₇PW₁₁O₃₉ and dispersed on quaternary ammonium functionalized chloromethylated polystyrene and employed as catalyst for oxidation of alcohols, but it required long reaction time 6 h to achieve 92% 1-phenylethanol conversion and 98.7% product selectivity with $2.56\text{mmol.g}^{-1}.\text{h}^{-1}$ specific activity. Therefore, the present catalyst was found to be the best choice for the oxidation of alcohols.

Catalyst recycling test

The reusability of the catalyst gained growing attention due to its great importance from both the industrial and academic points of view. The durability and recyclability of the fabricated catalyst for

oxidation of secondary alcohols was also assessed using the (1%)HRG/MnCO₃–(1%) ZrO_xcatalyst. The five recycle experiments were carried out under optimized conditions and the results were displayed in Fig. 10. After every single catalytic cycle, the solvent was evaporated, fresh toluene was added and the mixture was separated by simple centrifugation to recover the catalyst. The filtered solid is washed sequentially with toluene and the recovered catalyst was dried at 100°C for 4 h. The results revealed that, the as-fabricated catalyst can be recycled and reused

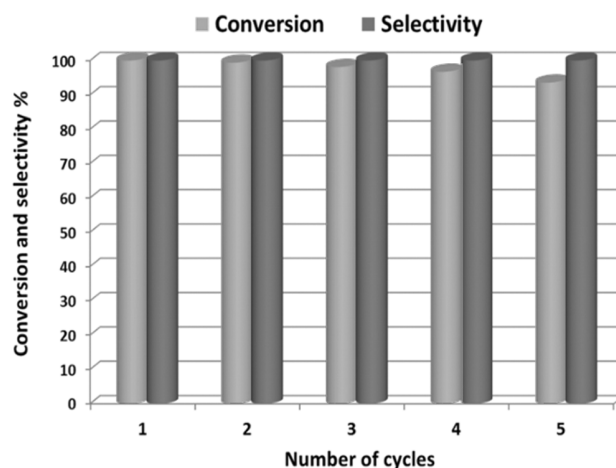


Fig. 10 — The reusability of (1%)HRG/MnCO₃–(1%)ZrO_x catalyst for the selective oxidation of 1-phenylethanol.(Reaction conditions: 2mmol of 1-phenylethanol, catalyst amount: 0.5 g, oxygen flow rate: 20 mL.min⁻¹, solvent: 10 mL of toluene, reaction temperature: 100°C and reaction time: 4 min).

Table 6 — Comparison of catalytic performance of (1%)HRG/MnCO₃–(1%)ZrO_x with reported catalysts for the oxidation of 1-phenylethanol.

Catalyst	Conv. (%)	Sel. (%)	T (°C)	Time	Sp. activity (mmol.g ⁻¹ .h ⁻¹)	Ref.
(1%)HRG/MnCO ₃ –(1%)ZrO _x	100	>99	100	4 min	60.0	This work
ZrO _x (1%)–MnCO ₃	100	>99	100	6 min	40.0	72
Au NPs/LDH	>99	>99.5	80	2 h	9.28	70
FeAPO–5	56.2	100	70	8 h	7.45	73
PW ₁₁ –DMA16/CMPS	92	98.7	80	6 h	2.56	71
Au–Pd/NaTNT	84	86	120	10 h	42.0	74
Pd–Au/LDH	>99	>99	80	1.5 h	6.70	75
Au/LDH	>99	>99.5	26	2 h	3.71	76
CuZnO	>99	>99	RT	3 h	33.33	77
2 wt% Ir/TiO ₂	>99	>99	80	3 h	2.67	78
Ru/CaO–ZrO _x	>99	>98	40	6 h	1.67	79
Pd/GC	18.9	>99.9	110	6 h	0.50	46
CoAl ₂ O ₄	63.45	83.25	80	8 h	0.79	15
Ag/ZnO	90	>99	100	6 h	30.0	80
Au/TiO ₂	100	>99	110	24 h	0.83	81
VOSO ₄ /TEMPO	99	96	80	2 h	37.78	82
CdS–MTA	40	>99	5	1.5 h	0.60	83

several times without obvious loss of activity and the selectivity to acetophenone is motionless (above 99%). During the five catalytic runs investigation, the alcohol conversion decreased from 100% to 93.58%, probably due to the loss of catalyst during the filtration method.⁴⁹ It can be said that the catalyst has a good reusability and stability.

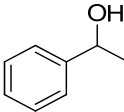
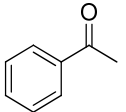
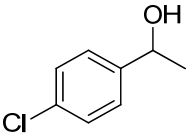
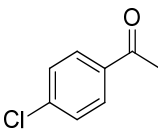
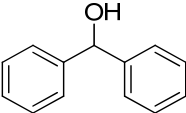
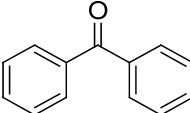
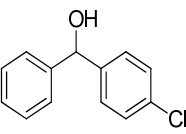
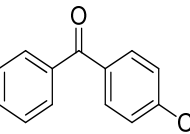
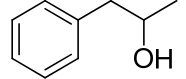
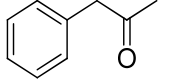
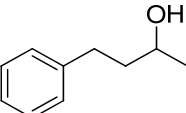
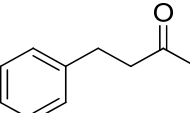
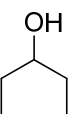
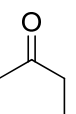
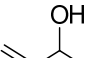
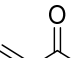
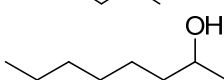
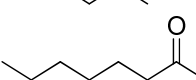
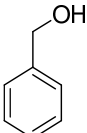
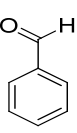
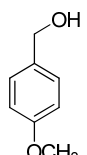
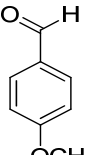
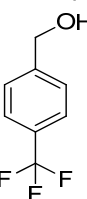
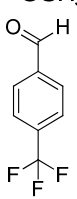
Oxidation of a variety of alcohols with molecular O₂ using (1%)HRG/MnCO₃-(1%)ZrO_x catalyst

In order to exploit the applicability of the prepared catalyst, aromatic and aliphatic secondary alcohols were selected for aerobic oxidation into corresponding carbonyl compounds i.e. ketones under the optimized conditions (Table 7, entries 1–9). The results for the oxidation of a wide range of alcohols are tabulated in Table 7. Obviously, all secondary benzylic alcohols were rapidly transformed to their corresponding ketones with complete conversion within short reaction times under optimal conditions (Table 7, entries 1–6). Moreover, an excellent selectivity (above 99%) toward corresponding ketones and aldehydes is observed for all the substrates and no by-products were found in the reaction mixture. The benzhydrol has converted to benzophenone with complete conversion within short reaction time of 5 min, while the complete oxidation of 4-chlorobenzhydrol took a slightly longer reaction time i.e. 7 min, this probably due to 4-chlorobenzhydrol contains electron withdrawing substituent that deactivate the aromatic ring by decreasing the electron density (Table 7, entries 3 and 4). Additionally, 1-phenylethanol and its derivatives also gave complete conversion and more than 99% selectivity in extremely short reaction times (Table 7, entries 1 and 2). Commonly, the oxidation of aliphatic alcohols is much more difficult than aromatic ones⁸⁴. The oxidation of secondary aliphatic alcohols to the corresponding ketones exhibited relatively lower catalytic activity by compared to secondary aromatic alcohols (Table 7, entries 7–9). For example, complete oxidation of 1-phenylethanol occurs after only 4 min, while the complete conversion of 2-octanol occurred within longer reaction period (100 min) (Table 7, entries 1 and 9).

In general, all primary aromatic alcohols have completely oxidized to their corresponding aldehydes in short reaction times (Table 7, entries 10–22). In addition, more than 99% aldehydes selectivity have achieved throughout all oxidation processes and no by-products were detected in the reaction mixture owing to no over-oxidation to carboxylic acids

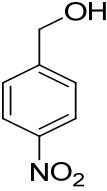
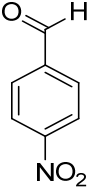
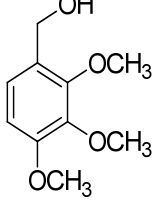
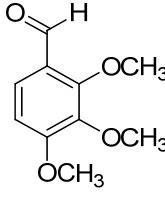
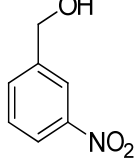
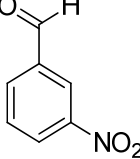
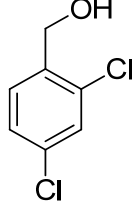
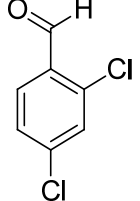
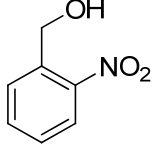
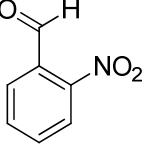
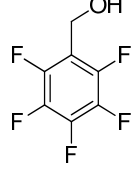
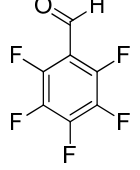
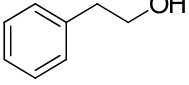
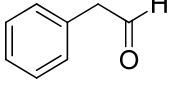
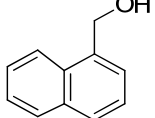
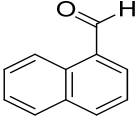
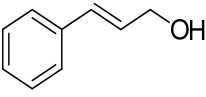
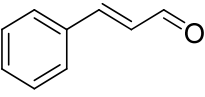
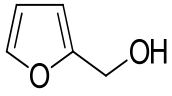
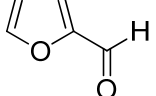
occurred. The oxidation of the benzyl alcohols was substantially effects by the electronic density of the substituents on the benzyl group. The oxidation of alcohols containing electron donating substituents into their corresponding aldehydes in complete conversions and less reaction times like 4-methoxybenzyl alcohol has fully oxidized into 4-methoxybenzaldehyde within only 4 min (Table 7, entry 11), as electron releasing groups are known to activate the benzyl alcohols. In contrast, the electron withdrawing groups are considered to be deactivating the aromatic ring in oxidation process which causes slightly decreases the oxidation rate and required longer reaction time such as 4-nitrobenzyl alcohol exhibited 100% conversion after longer reaction time (12 min) (Table 7, entry 13)⁸⁵. On the other hand, *ortho*-substituted alcohols oxidized slowly and gave complete conversions within longer times as compared to *meta*- and *para*-substituted alcohols, which may be possibly due to *ortho*- position has maximum steric hindrance by compared to other positions⁸⁶. For instance, *ortho*-nitrobenzyl alcohol was completely converted to its corresponding aldehyde after 13 min (Table 7, entry 17), while for *para*- and *meta*-nitrobenzyl alcohol were fully oxidized within shorter time 8 and 11 min, respectively (Table 7, entries 13 and 15). It was observed that the performance of the oxidation reaction decreases with an increase in the bulkiness of the substituent. This probably owing to the steric hindrance impede the oxidation of the bulky alcohols such as (4-CF₃, 2,3,4-TriOMe, 2,4-DiCl, and 2,3,4,5,6-Pentafluoro) (Table 7, entries 12,14,16,18)²³. The oxidation of allylic alcohols like cinnamyl alcohol also rapidly converted to give cinnamaldehyde in complete conversion with more than 99% product selectivity after short reaction time 11 min (Table 7, entry 21). Furfuryl alcohol as example for a heteroaromatic alcohol has also converted completely to furfural was achieved in 20 min (Table 7, entry 22). The prepared catalyst showed good activity for the selective oxidation of primary aliphatic alcohols into their corresponding aldehydes under the identical circumstances (Table 7, entries 23–26). For example, the oxidation of cyclohexanemethanol, 5-Hexen-1-ol, octan-1-ol, and citronellol to corresponding aldehydes takes place in relatively longer reaction periods by compared to aromatic ones (Table 7, entries 23–26). Eventually, it can be concluded that the aerobic oxidation of alcohols in presence of (1%)HRG/ MnCO₃-(1%)ZrO_x catalyst has strongly influenced by two factors, electronic and steric effects.

Table 7 — Catalytic oxidation of various alcohols by molecular O₂ in presence of (1%)HRG/MnCO₃–(1%)ZrO_x catalyst. (Contd.)

Entry	Alcohol	Product	Time (min)	Conv. (%)	Sel. (%)
1			4	100	>99
2			6	100	>99
3			5	100	>99
4			7	100	>99
5			11	100	>99
6			16	100	>99
7			35	100	>99
8			85	100	>99
9			100	100	>99
10			4	100	>99
11			4	100	>99
12			7	100	>99

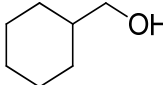
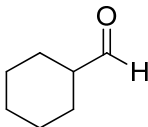
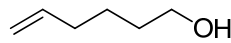
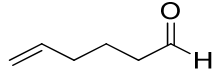
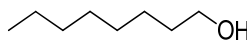
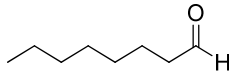
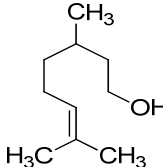
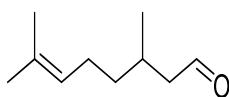
(Contd.)

Table 7 — Catalytic oxidation of various alcohols by molecular O₂ in presence of (1%)HRG/MnCO₃-(1%)ZrO_x catalyst. (*Contd.*)

Entry	Alcohol	Product	Time (min)	Conv. (%)	Sel. (%)
13			8	100	>99
14			7	100	>99
15			11	100	>99
16			12	100	>99
17			13	100	>99
18			15	100	>99
19			14	100	>99
20			25	100	>99
21			11	100	>99
22			20	100	>99

(Contd.)

Table 7 — Catalytic oxidation of various alcohols by molecular O₂ in presence of (1%)HRG/MnCO₃–(1%)ZrO_x catalyst.

Entry	Alcohol	Product	Time (min)	Conv. (%)	Sel. (%)
23			40	100	>99
24			90	100	>99
25			85	100	>99
26			80	100	>99

Reaction conditions: catalyst: (1%)HRG/MnCO₃–(1%)ZrO_x, 2 mmol of alcohol, catalyst amount: 0.5 g, calcination temperature: 300°C, oxygen flow rate: 20 mL.min⁻¹, solvent: 10 mL of toluene, and reaction temperature: 100°C.

Conclusion

In summary, ZrO_xNPs doped MnCO₃ supported on highly reduced graphene composite was found to be as an efficient, cheap, and recyclable catalyst for oxidation of alcohols to their corresponding carbonyl derivatives with molecular O₂ as eco-friendly oxidant without using any additive or base. Interestingly, the catalytic activity of ZrO_x NPs doped MnCO₃ catalyst has markedly enhanced after using carbon support for the selective alcohol oxidation. A complete conversion of 1-phenylethanol and acetophenone selectivity were achieved within extremely short reaction time along with 60.0 mmol.g⁻¹.h⁻¹ specific activity. To the best of our knowledge, the obtained specific activity is much higher than the previously reported in earlier publications. Moreover, the present catalyst exhibited an efficient catalytic performance for the oxidation of various aromatic, aliphatic, allylic, heteroatomic, primary and secondary alcohols within relatively short reaction times under mild reaction conditions. Additionally, the product selectivity is very high (>99%) have achieved for all alcohols used in the present work. Moreover, the as-prepared catalyst can be recovered and reused five times without manifest loss of catalytic performance and the selectivity remained almost unchanged. The obvious advantages of the present catalytic protocol are: (a) simple work-up approach; (b) ecologically friendly oxidant; (c) no additives or bases are required for the oxidation process; (d) complete conversion of all types of alcohols; (e) excellent product

selectivities; (f) extremely rapid reaction; (g) very mild reaction conditions and (h) easy reusable catalyst. All these features will give rise to the present catalytic system to be very much useful and applicable for the oxidation of alcohols.

Acknowledgement

The authors extend their appreciation to the Deanship of Scientific Research at King Saud University for funding this work through the research group project No. RG-1436-032.

References

- Dimitratos N, Lopez-Sanchez J A & Hutchings G J, *Chem Sci*, 3 (2012) 20.
- Liu K, Chen T, Hou Z, Wang Y & Dai L, *Catal Lett*, 144 (2014) 314.
- Parmeggiani C & Cardona F, *Green Chem*, 14 (2012) 547.
- Guo Z, Liu B, Zhang Q, Deng W, Wang Y & Yang Y, *Chem Soc Rev*, 43 (2014) 3480.
- Liu K, Chen Z, Hou Z, Wang Y & Dai L, *Catal Lett*, 144 (2014) 935.
- Zhao G, Hu H, Deng M & Lu Y, *Chem Commun*, 47 (2011) 9642.
- Ma C Y, Dou B J, Li J J, Cheng J, Hu Q, Hao Z P & Qiao S Z, *Appl Catal B: Environ*, 92 (2009) 202.
- Wang T, Yuan X, Li S, Zeng L & Gong J, *Nanoscale*, 7 (2015) 7593.
- Yan Y, Jia X & Yang Y, *Catal Today*, 259 (2016) 292.
- Li G, Jiang L, Zhang B, Jiang Q, Sheng Su D & Sun G, *Int J Hydrogen Energy*, 38 (2013) 12767.
- Mondelli C, Ferri D & Baiker A, *J Catal*, 258 (2008) 170.
- Wusiman A & Lu C D, *Appl Organomet Chem*, 29 (2015) 254.
- Xie M, Dai X, Meng S, Fu X & Chen S, *Chem Eng J*, 245 (2014) 107.

- 14 Cruz P, Pérez Y, del Hierro I & Fajardo M, *Microporous Mesoporous Mater*, 220 (2016) 136.
- 15 Ragupathi C, Vijaya J J, Narayanan S, Jesudoss S & Kennedy L J, *Ceram Int*, 41 (2015) 2069.
- 16 Hajipour A R, Karimi H & Koochi A, *Chin J Catal*, 36 (2015) 1109.
- 17 Cang R, Lu B, Li X, Niu R, Zhao J & Cai Q, *Chem Eng Sci*, 137 (2015) 268.
- 18 Behera G C & Parida K, *Appl Catal A*, 413 (2012) 245.
- 19 Adil S, Assal M, Khan M, Al-Warthan A & Siddiqui M R H, *Oxid Commun*, 36 (2013) 778.
- 20 Noshiranzadeh N, Bikas R, Ślepokura K, Mayeli M & Lis T, *Inorg Chim Acta*, 421 (2014) 176.
- 21 Rao P S N, Rao K T V, Prasad P S S & Lingaiah N, *Chin J Catal*, 32 (2011) 1719.
- 22 Sousa S C, Bernardo J R, Florindo P R & Fernandes A C, *Catal Commun*, 40 (2013) 134.
- 23 Meng S, Ye X, Ning X, Xie M, Fu X & Chen S, *Appl Catal B: Environ*, 182 (2016) 356.
- 24 Borthakur R, Asthana M, Kumar A & Lal R A, *Inorg Chem Commun*, 46 (2014) 198.
- 25 Arena F, Gumina B, Lombardo A F, Espro C, Patti A, Spadaro L & Spiccia L, *Appl Catal B: Environ*, 162 (2015) 260.
- 26 Mahdavi V & Mardani M, *Mater Chem Phys*, 155 (2015) 136.
- 27 Clarke T J, Kondrat S A & Taylor S H, *Catal Today*, 258 (2015) 610.
- 28 Guo X, Li J & Zhou R, *Fuel*, 163 (2016) 56.
- 29 Kim S C, Park Y-K & Nah J W, *Powder Technol*, 266 (2014) 292.
- 30 Piumetti M, Fino D & Russo N, *Appl Catal B: Environ*, 163 (2015) 277.
- 31 Feng Z, Xie Y, Hao F, Liu P & Luo H a, *J Mol Catal A: Chem*, 410 (2015) 221.
- 32 Burange A S, Kale S R & Jayaram R V, *Tetrahedron Lett*, 53 (2012) 2989.
- 33 Pei J, Han X & Lu Y, *Build Environ*, 84 (2015) 134.
- 34 Liao L, Peng H & Liu Z, *J Am Chem Soc*, 136 (2014) 12194.
- 35 Novoselov K S, Geim A K, Morozov S V, Jiang D, Zhang Y, Dubonos S V, Grigorieva I V & Firsov A A, *Science*, 306 (2004) 666.
- 36 Zhao L, Li H, Gao S, Li M, Xu S, Li C, Guo W, Qu C & Yang B, *Electrochim Acta*, 168 (2015) 191.
- 37 Qiu B, Xing M & Zhang J, *J Am Chem Soc*, 136 (2014) 5852.
- 38 Cheng J, Wang B, Xin H L, Yang G, Cai H, Nie F & Huang H, *J Mater Chem:A*, 1 (2013) 10814.
- 39 Scheuermann G M, Rumi L, Steurer P, Bannwarth W & Mühlaupt R, *J Am Chem Soc*, 131 (2009) 8262.
- 40 Rana S, Maddila S, Yalagala K & Jonnalagadda S B, *Appl Catal A*, 505 (2015) 539.
- 41 Mirza-Aghayan M, Tavana M M & Boukherroub R, *Catal Commun*, 69 (2015) 97.
- 42 Metin Ö, Kayhan E, Özkar S & Schneider J J, *Int J Hydrogen Energy*, 37 (2012) 8161.
- 43 Li Y, Yu Y, Wang J-G, Song J, Li Q, Dong M & Liu C-J, *Appl Catal B: Environ*, 125 (2012) 189.
- 44 Qusti A, Mohamed R & Salam M A, *Ceram Int*, 40 (2014) 5539.
- 45 Xie W, Zhang F, Wang Z, Yang M, Xia J, Gui R & Xia Y, *J Electroanal Chem*, 761 (2016) 55.
- 46 Wu G, Wang X, Guan N & Li L, *Appl Catal B: Environ*, 136 (2013) 177.
- 47 Kadam M M, Dhopte K B, Jha N, Gaikar V G & Nemade P R, *New J Chem*, 40 (2016) 1436.
- 48 Zahed B & Hosseini-Monfared H, *Appl Surf Sci*, 328 (2015) 536.
- 49 Yu X, Huo Y, Yang J, Chang S, Ma Y & Huang W, *Appl Surf Sci*, 280 (2013) 450.
- 50 Li F, Guo Y, Wu T, Liu Y, Wang W & Gao J, *Electrochim Acta*, 111 (2013) 614.
- 51 Wu S, He Q, Zhou C, Qi X, Huang X, Yin Z, Yang Y & Zhang H, *Nanoscale*, 4 (2012) 2478.
- 52 Yang M-Q, Zhang N & Xu Y-J, *ACS Appl Mater Interfaces*, 5 (2013) 1156.
- 53 Siddiqui M R H, Warad I, Adil S, Mahfouz R & Al-Arifi A, *Oxid Commun*, 35 (2012) 476.
- 54 Alabbad S, Adil S, Assal M, Khan M, Alwarthan A & Siddiqui M R H, *Arab J Chem*, 7 (2014) 1192.
- 55 Adil S F, Alabbad S, Kuniyil M, Khan M, Alwarthan A, Mohri N, Tremel W, Tahir M N & Siddiqui M R H, *Nanoscale Res Lett*, 10 (2015) 52.
- 56 Hummers Jr W S & Offeman R E, *J Am Chem Soc*, 80 (1958) 1339.
- 57 Wang Y, Zhao Y, He W, Yin J & Su Y, *Thin Solid Films*, 544 (2013) 88.
- 58 Geng L, Wu S, Zou Y, Jia M, Zhang W, Yan W & Liu G, *J Colloid Interface Sci*, 421 (2014) 71.
- 59 Miao M, Feng J, Jin Q, He Y, Liu Y, Du Y, Zhang N & Li D, *RSC Adv*, 5 (2015) 36066.
- 60 Wojtoniszak M & Mijowska E, *J Nanopart Res*, 14 (2012) 1248.
- 61 Stankovich S, Piner R D, Nguyen S T & Ruoff R S, *Carbon*, 44 (2006) 3342.
- 62 Zhou J, Wang Y, Guo X, Mao J & Zhang S, *Green Chem*, 16 (2014) 4669.
- 63 Shen J, Shi M, Li N, Yan B, Ma H, Hu Y & Ye M, *Nano Res*, 3 (2010) 339.
- 64 Santra S, Hota P K, Bhattacharyya R, Bera P, Ghosh P & Mandal S K, *ACS Catal*, 3 (2013) 2776.
- 65 Qiu T, Wang J, Lu Y & Yang W, *RSC Adv*, 4 (2014) 23027.
- 66 Gurunathan S, Han J W, Eppakayala V & Kim J-H, *Colloids Surf B*, 102 (2013) 772.
- 67 Al-Marri A H, Khan M, Shaik M R, Mohri N, Adil S F, Kuniyil M, Alkathlan H Z, Al-Warthan A, Tremel W & Tahir M N, *Arab J Chem*, 9 (2016) 835.
- 68 Assal M E, Kuniyil M, Khan M, Al Warthan A, Siddiqui M R H, Tremel W, Nawaz Tahir M & Adil S F, *Chem Open*, (2016)
- 69 Zhan G, Hong Y, Mbah V T, Huang J, Ibrahim A-R, Du M & Li Q, *Appl Catal A*, 439 (2012) 179.
- 70 Liang W, Xiangju M & Fengshou X, *Chin J Catal*, 31 (2010) 943.
- 71 Wang H, Fang L, Yang Y, Hu R & Wang Y, *Appl Catal A*, 520 (2016) 35.
- 72 Assal M E, Kuniyil M, Khan M, Shaik M R, Al-Warthan A, Siddiqui M R H, Labis J P & Adil S F, *Adv Mater Sci Eng*, 2017 (2017)

- 73 Qi L, Qi X, Wang J & Zheng L, *Catal Commun*, 16 (2011) 225.
- 74 Nepak D & Darbha S, *Catal Commun*, 58 (2015) 149.
- 75 Shi Y, Yang H, Zhao X, Cao T, Chen J, Zhu W, Yu Y & Hou Z, *Catal Commun*, 18 (2012) 142.
- 76 Wang L, Zhang J, Meng X, Zheng D & Xiao F-S, *Catal Today*, 175 (2011) 404.
- 77 Forouzani M, Mardani H R, Ziari M, Malekzadeh A & Biparva P, *Chem Eng J*, 275 (2015) 220.
- 78 Yoshida A, Mori Y, Ikeda T, Azemoto K & Naito S, *Catal Today*, 203 (2013) 153.
- 79 Yasu-eda T, Kitamura S, Ikenaga N-o, Miyake T & Suzuki T, *J Mol Catal A: Chem*, 323 (2010) 7.
- 80 Hosseini-Sarvari M, Ataee-Kachouei T & Moeini F, *Mater Res Bull*, 72 (2015) 98.
- 81 Vindigni F, Dughera S, Armigliato F & Chiorino A, *Monatsh Chem*, 147 (2016) 391.
- 82 Du Z, Ma J, Ma H, Wang M, Huang Y & Xu J, *Catal Commun*, 11 (2010) 732.
- 83 Tamiolakis I, Lykakis I N & Armatas G S, *Catal Today*, 250 (2015) 180.
- 84 Olgún J, Müller-Bunz H & Albrecht M, *Chem Commun*, 50 (2014) 3488.
- 85 Hasannia S & Yadollahi B, *Polyhedron*, 99 (2015) 260.
- 86 Kadam M M, Dhopte K B, Jha N, Gaikar V G & Nemade P R, *J Chem*, 40 (2016) 1436.